

Research papers

Towards a soil moisture drought monitoring system for South Korea



Hahn Chul Jung^{a,b,*}, Do-Hyuk Kang^{a,c}, Edward Kim^a, Augusto Getirana^{a,c}, Yeosang Yoon^{a,d}, Sujay Kumar^a, Christa D. Peters-lidard^e, EuiHo Hwang^f

^a Hydrological Sciences Laboratory, NASA Goddard Space Flight Center, Greenbelt, MD, USA

^b Korea Ocean Satellite Center, Korea Institute of Ocean Science and Technology, Busan, South Korea

^c Earth System Science Interdisciplinary Center, University of Maryland, College Park, MD, USA

^d Science Applications International Corporation, Reston, VA, USA

^e Earth Science Division, NASA Goddard Space Flight Center, Greenbelt, MD, USA

^f Water Resources Satellite Research Center, K-water Institute, K-water, Daejeon, South Korea

ARTICLE INFO

This manuscript was handled by Emmanouil Anagnostou, Editor-in-Chief, with the assistance of Viviana Maggioni, Associate Editor

Keywords:

Agricultural drought

Soil moisture

Precipitation

Land surface model

ABSTRACT

The Korea Land Data Assimilation System (KLDAS) has been established for agricultural drought (i.e. soil moisture deficit) monitoring in South Korea, running the Noah-MP land surface model within the NASA Land Information System (LIS) framework with the added value of local precipitation forcing dataset and soil texture maps. KLDAS soil moisture is benchmarked against three global products: the Global Land Data Assimilation System (GLDAS), the Famine Early Warning Systems Network (FEWS NET) Land Data Assimilation System (FLDAS), and the European Space Agency Climate Change Initiative (ESA CCI) satellite product. The evaluation is performed using in situ measurements for 2013–2015 and one month standardized precipitation index (SPI-1) for 1982–2016, focusing on four major river basins in South Korea. The KLDAS outperforms all benchmark products in capturing soil moisture states and variability at a basin scale. Compared to GLDAS and FLDAS products, the EAS CCI product is not feasible for long term agricultural monitoring due to lower data quality for early periods (1979–1991) of soil moisture estimates. KLDAS shows that the most recent 2015 drought event leads to highest drought areas in the Han and Geum River basins in the past 35 years. This work supports KLDAS as an effective agricultural drought monitoring system to provide continuous regional high-resolution soil moisture estimates in South Korea.

1. Introduction

Drought is commonly characterized by the deficits of hydrologic budget variables (i.e. precipitation, soil moisture, groundwater, evapotranspiration and streamflow) from average conditions (Anderson et al., 2013; Kumar et al., 2014). Drought can develop into a natural disaster, depending on its severity, duration and frequency, which leads to an increased need for drought monitoring and water resource management systems (Anderson et al., 2011, 2013). Under the East Asian monsoonal circulation, the Korean peninsula has been experiencing a 4–6-year cycle of extreme droughts at a nationwide scale since 1960 (Kwon et al., 2016). South Korea recently faced a severe drought during 2014–2015 when the annual rainfall was less than half of the historical average for two consecutive years, which was regarded as the worst drought in the past 50 years (Kwon et al., 2016; Hong et al., 2016). That drought resulted in the lowest recorded water level of most multipurpose dams and downstream reservoirs nearly depleted as a result of

the decreased inflow in the Han River and Geum River basins over northern and western South Korea (Kwon et al., 2016; Hong et al., 2016). The 2014–2015 drought also ruined ~60 km² of agricultural area, including ~25 km² of rice paddies equivalent to 0.3% of total rice paddy area (Hong et al., 2016). Currently, the need for a national-level drought monitoring system has received considerable attention and efforts are being made to improve the early detection of drought and the efficiency of mitigation responses (Jang, 2018). The decision making for drought mitigation in South Korea has been mainly supported by a dense network of rainfall data in meteorological stations and water storage in agricultural reservoirs. The current actions and measures in the drought system have been carried out based on a meteorological drought index considering precipitation deficit, water supply and demand. However, there has been no attempt to produce spatially distributed hydrological drought indices with the state-of-the-art land surface models, reporting an agricultural drought (i.e. deficit in soil moisture states) over South Korea.

* Corresponding author at: 385 Haeyang-ro Yeongdo-gu, Busan, South Korea.
E-mail address: hahnchul.jung@kiost.ac.kr (H.C. Jung).

Soil moisture plays an important role in our understanding of the interaction between the atmosphere and Earth's surface and reflects agricultural and hydrological drought conditions (Sheffield and Wood, 2007; Spennemann et al., 2015; Li et al., 2018). Compared to precipitation, soil moisture is more spatially heterogeneous and an excellent proxy indicator to represent local drought conditions controlled by topography and land cover (Chaney et al., 2015). Recently, in situ measurements and remote sensing products have provided soil moisture estimation, which can serve as important short-term drought (monthly to seasonal) indicators (Spennemann et al., 2015). But, long term (> 30 years) records of soil moisture measurements in their spatial and temporal coverages are not available in many parts of the world to represent the average conditions and figure out the extremes (Anderson et al., 2011; Spennemann et al., 2015). Remote sensing instruments have been important to provide spatiotemporally continuous soil moisture for agricultural drought monitoring since the 1970 s (Jackson et al., 2010; Pietroniro and Prowse, 2002). But, their coarse spatial scales and limited operation period of these satellite sensors have prevented their widespread application in drought monitoring. For studying long term trend and variability of soil moisture, the European Space Agency Climate Change Initiative (ESA CCI) combined multiple passive and active microwave soil moisture satellite products along with a consistent climatology (Loew et al., 2013; Dorigo et al., 2015).

Several studies have demonstrated that the use of land surface models (LSMs) driven by observed meteorological forcing datasets produce spatially and temporally continuous estimation of agricultural drought across scales. At a global scale, the Global Land Data Assimilation System (GLDAS) provides products related to soil moisture and drought conditions in near real time from multiple LSMs and different meteorological forcing datasets at 1° resolution for version 1 and 0.25° resolutions for version 2 products (Rodell et al., 2004). Other studies focused on agricultural droughts in South America (e.g. Spennemann et al., 2015) and China (e.g. Yuan et al., 2015) from GLDAS, the United States (e.g. Kumar et al., 2014) from the North American Land Data Assimilation System (NLDAS; Mitchell et al., 2004), and Africa (e.g. McNally et al., 2016) from the Famine Early Warning Systems Network (FEWS NET) Land Data Assimilation System (FLDAS) (McNally et al., 2017). However, few studies have attempted to use LSMs and investigate agricultural drought over South Korea where high resolution soil moisture data are necessary to identify detailed spatial drought conditions due to complex topography and heterogeneous soil moisture texture types (Park et al., 2017). For instance, though GLDAS version 2 products can represent most inland areas in South Korea with an intermediate spatial resolution (~25 km), GLDAS version 1 products (including simulations of multiple LSMs) and passive microwave products (i.e. SMMR, SSM/I and TMI) with a coarse spatial resolution (60–100 km) are limited to capture the complete coverage of South Korea, excluding most coastal regions of the Korean Peninsula.

Model-based soil moisture has not been fully served as an agricultural drought index in South Korea where rice paddy agriculture is an important sector as a major source of livelihood similar to South and Southeast Asian countries. Most of the agricultural drought analysis in South Korea have been carried out using remote sensing data and reanalysis data without a modeling framework (e.g. Ryu et al., 2019; Yoon et al., 2020; Park et al., 2017; Sur et al., 2015). Therefore, this study (1) establishes the Korea Land Data Assimilation System (KLDAS) with the added value of local precipitation forcing dataset and soil texture maps to produce soil moisture estimates and their drought estimates at a 1-km spatial resolution; (2) evaluates soil moisture estimates and drought estimates from KLDAS against in situ measurements for 2013–2015 and the one month standardized precipitation index (SPI-1) for 1982–2016; (3) compares KLDAS products with two benchmark LDAS products (GLDAS version 2 and FLDAS) and one remote sensing product (ESA CCI); and (4) examines the performance of KLDAS agricultural drought area percentages in the four major river

basins of South Korea. The focus here is to evaluate surface soil moisture estimates due to the data availability of the remote sensing product and in situ measurements, though agriculture drought is more related to shortages of root zone soil moisture. This study serves to support the use of KLDAS as an agricultural drought indicator to facilitate continuous regional high resolution soil moisture monitoring for the analysis of droughts over South Korea. The findings of this study serves as an important baseline and support for the upcoming KLDAS development driven by a broad range of improved local meteorological forcing datasets.

2. Data and methods

2.1. Study area

The study area covers the southern part of the Korean peninsula between 33.8° N to 39° N and 124.5° E to 130° E. Climatologically, this domain represents the Asian monsoon region, which has a wet summer season from June to August when nearly half of the annual precipitation of 1350 mm falls with summer typhoons and heavy rains (Jang, 2018; Sur et al., 2015). The country frequently experiences droughts during crop growing seasons between April and October due to absolute shortage of rainfall (Park et al., 2017). Over 60% of the domain consists of mixed forest, deciduous broadleaf forest, and woody savanna whereas cropland covers 30% mainly over the western and southwestern regions (Sur et al., 2015). The agriculture area of South Korea is ~ 16,000 km² (MAFRA, 2017). Agricultural reservoirs (~17,000), groundwater pumping stations (~7,000), irrigation canals (~120,000 km²) serve to offer water to the cropland (Ryu et al., 2019; MAFRA, 2017). This study focuses on the four major river basins which current national drought management framework has been mainly oriented to: Han River basin (~26,000 km²) over north, Geum River basin (~10,000 km²) over west, Nakdong River basin (~24,000 km²) over southeast, and Yeongsan River basin (~8,000 km²) over southwest of South Korea (~100,000 km²).

2.2. Kldas

KLDAS was established using the Noah land surface model with Multi-Parameterization, version 3.6 (Noah-MP; Cai et al., 2014) at a 0.01° spatial resolution grid with a 15-min timestep to generate daily energy and water balance variables. The KLDAS domain covers the Korean peninsula, including North and South Korea, between 33° N to 44° N and 124° E to 132° E. Noah-MP was selected because of its ability to explicitly represent groundwater, dynamic vegetation phenology, and a multilayer snowpack. In this study, we used the modified International Geosphere Biosphere Programme 20-category landuse data from the Moderate Resolution Imaging Spectroradiometer (MODIS; Friedl et al., 2002), monthly climatologies of leaf area index (LAI) and greenness fraction from the NOAA Advanced Very High Resolution Radiometer (AVHRR; Gutman and Ignatov, 1998). For model physical processes, we used the simple groundwater model (SIMGM) runoff and groundwater option, monthly LAI with constant shade fraction for vegetation model and the Ball-Berry for canopy stomatal resistance (Niu et al., 2007). We ran the simulation from 1980 to 2016 and reinitialized it in 1980 for the LSM variables to reach equilibrium. Soil moisture estimates from the first soil layer (0–10 cm) out of four soil layers were extracted for our analysis. The choice of the soil depth was matched with the average soil layer depth of in situ measurements used in this study as well as GLDAS and FLDAS products.

The Modern-Era Retrospective analysis for Research and Applications, version 2 (MERRA-2; Reichle et al., 2017) datasets were used to force the model. MERRA-2 is available globally at the hourly time step and horizontal resolution of 2/3° longitude by 1/2° latitude. Specifically, precipitation observations from 101 Automated Synoptic Observing System (ASOS) stations of Korean Meteorological

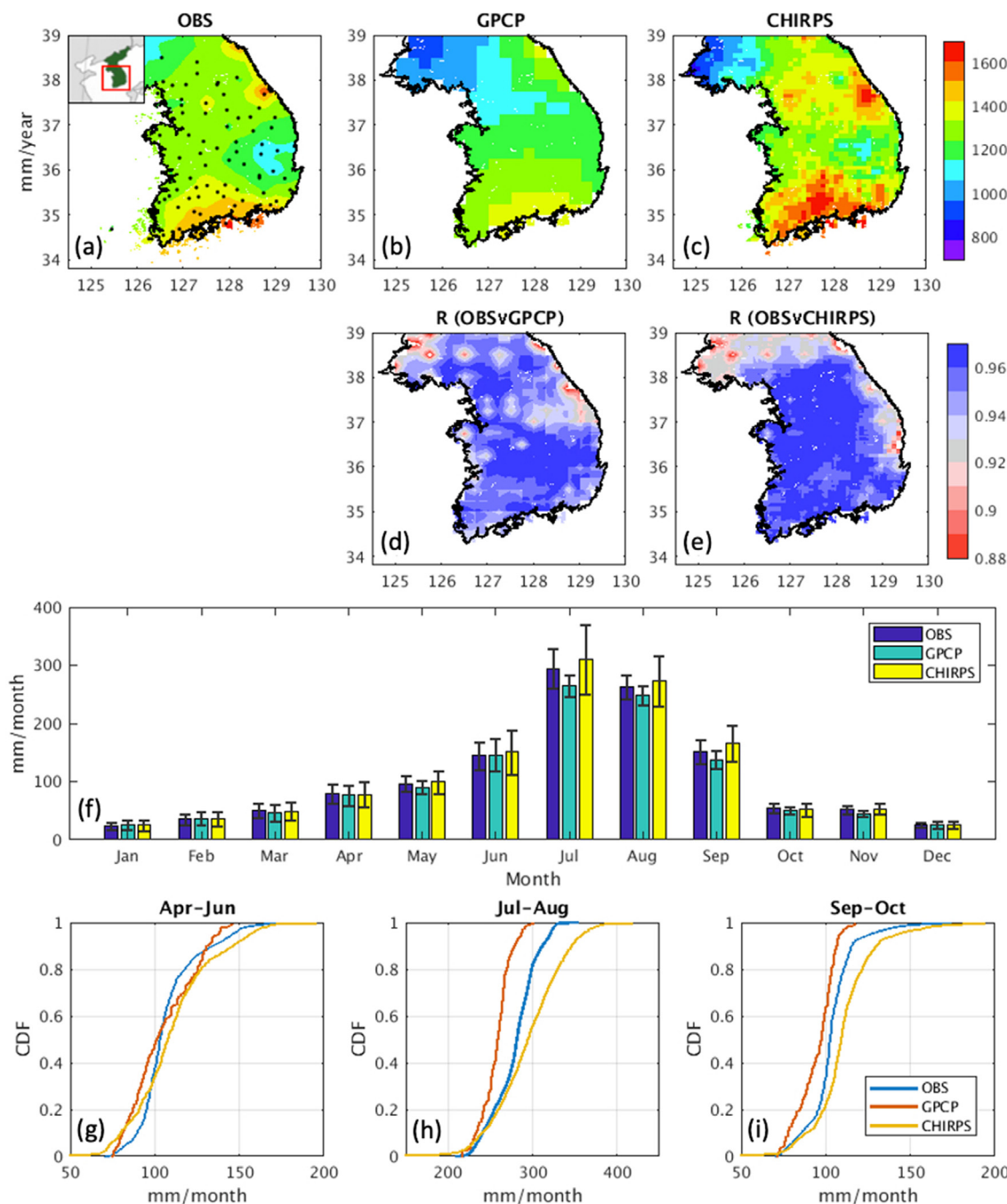


Fig. 1. Spatial distribution maps of (a) ASOS observation (OBS), (b) GPCP, and (c) CHIRPS annual precipitation (mm/year) for the period 1982–2016. (a) Black dots indicate locations of the precipitation measurement sites. Temporal correlation coefficients (R) of (d) OBSvGPCP and (e) OBSvCHIRPS. (f) Average monthly precipitation rates of each of three precipitation datasets. Cumulative distribution function (CDF) for monthly precipitation rates from (g) April to June, (h) July to August, and (i) September to October.

Administration (KMA) in South Korea and 27 Global Telecommunication System (GTS) stations in North Korea were processed into 12 hourly and 0.01° gridded data using inverse distance weighting. Locations of the ASOS stations used in this study are shown in Fig. 1a. The combined ASOS and GTS precipitation dataset replaced the MERRA-2 precipitation fields. The elevation data from the Shuttle Radar Topography Mission (SRTM; Rodriguez et al., 2005) was used to derive the topography datasets of elevation, slope, and aspect. Other meteorological inputs (i.e. air temperature, humidity, pressure, winds, radiation) from MERRA-2 were adjusted for the elevation differences through lapse-rate and slope-aspect correction methods (Kumar et al., 2013) and downscaled to 0.01° gridded data. Instead of employing

global soil texture datasets, 16-category soil texture maps at a 30-meter spatial resolution grid over South Korea, combined with 8-category soil texture maps at a scale of 1:500,000 for the border between North and South Korea, from the Korea Water Resources Corporation (K-water; more details can be found in Jung et al., 2017), were rescaled into 0.01° gridded data as inputs to the KLDAS. Over 70% of the soil type consists of sand and loam which are more dominant than clay and silt in the study area.

2.3. Comparison datasets

2.3.1. Gldas

The soil moisture products from GLDAS, version 2.0 (1948–2010) and version 2.1 (2000-present) datasets from the Noah version 3.3 model on a 0.25° gridded data were used in this study (Rodell et al., 2004). In contrast to the same LSM used in the two versions, GLDAS-2.0 was entirely forced with the Princeton meteorological forcing data on a 1° gridded data (Sheffield et al., 2006) whereas GLDAS-2.1 was forced with a combination of National Center for Environmental Prediction's Global Data Assimilation System (GDAS) atmospheric analysis fields on a 0.2° gridded data (Derber et al., 1991) and Global Precipitation Climatology Project (GPCP) precipitation field on a 1° gridded data (Adler et al., 2003). GLDAS version 2.1 starts in January 2000, so the bias-corrected GLDAS version 2.0 for years 1982–1999 are merged into GLDAS version 2.1 to match the long term KLDAS outputs for 1982–2016. We used the mean and standard deviation of the two version datasets during the overlapped years 2000–2010 to correct the bias between the two products. The soil texture maps were derived from 5 min resolution global soil datasets with 16-category soil texture of Food and Agriculture Organization of the United Nations (FAO; more details can be found in Reynolds et al., 2000; Rodell et al., 2004). The global soil texture map shows a constant class of loam in the study area.

2.3.2. Fldas

FLDAS recently released global monthly products in 0.10° resolution from the Noah version 3.6.1 model, ranging from January 1982 to present (McNally et al., 2017). The soil moisture estimates in the first layer (0–10 cm) from the FLDAS products were used for this study. The simulation was forced by a combination of the MERRA-2 data and Climate Hazards Group InfraRed Precipitation with Station (CHIRPS; Funk et al., 2015) 6-hourly rainfall data. Note that compared to spatial resolution differences amongst the three LDAS products, the FAO's global soil texture maps (used in GLDAS) and the MERRA-2 meteorological forcing dataset (used in KLDAS) were rescaling into 0.10° gridded data to inputs to the FLDAS.

2.3.3. EsA CCI

The ESA CCI surface soil moisture dataset version 4.2 from November 1978 to December 2016 was used in this study (Dorigo et al., 2015). The global product combined satellite soil moisture retrievals from four passive (i.e. the Nimbus 7 Scanning Multi-channel Microwave Radiometer (SMMR), the Special Sensor Microwave Imagers (SSM/I) of the defense meteorological satellite program, the Tropical Rainfall Measuring Mission Microwave Imager (TMI), and the Advanced Microwave Scanning Radiometer-Earth Observing System (AMSR-E) sensor on NASA's Aqua satellite) and two active (the European Remote Sensing Satellites 1 and 2 Active Microwave Instrument (AMI) wind scatterometer and the Advanced Scatterometer (ASCAT) onboard the meteorological operational platform). The active products were merged into a combined dataset since August 1991. This long term product enables climate studies and drought analysis, which is available daily on a 0.25° spatial resolution on a global coverage.

2.4. Evaluation procedure

We evaluate KLDAS soil moisture estimates for the use of drought monitoring during the crop growing seasons from April to October. Also, we employ GLDAS, FLDAS and ESA CCI as benchmark datasets and intercompare them with KLDAS. These benchmark products were downscaled into 0.01° using nearest neighbor interpolation for our evaluation and comparison.

First, precipitation datasets GPCP (used to force GLDAS) and CHIRPS (used to force FLDAS) were evaluated against the ASOS gridded dataset (used in KLDAS) for years 1982–2016. Since precipitation is the most important input data into the LSMs to estimate soil moisture, we

calculated their spatial distribution maps of annual rates, the average monthly rates, and the cumulative distribution functions (CDF) for monthly precipitation during crop growing seasons.

Second, soil moisture estimates were evaluated against 78 in situ observations for short term 3 years, 2013–2015. There are 17 stations used for evaluation in the Han River basin, 19 in the Geum River basin, 13 in the Nakdong River basin, and 9 in the Yeongsan River basin. Daily soil moisture observations were obtained from the Korea Meteorological Administration (KMA) and Rural Development Administration (RDA) and were aggregated into monthly values for the evaluation (more details can be found in Jung et al., 2017). At the stations, soil moisture was measured using Time Domain Reflectometry (TDR) at an average depth of 10 cm. Though the sensing depth of satellite data (e.g. ESA CCI) is only a few centimeters, surface soil moisture is closely related to soil moisture in the upper 10 cm (Albergel et al., 2008), which is the depth of the first soil layer for our selected LSMs in this study. Considering that there are large biases between the model and satellite soil moisture datasets (Koster et al., 2009), we computed anomalies for all soil moisture values. The Pearson correlation coefficient (R) and the root-mean-squared-error (RMSE) of the soil moisture anomalies were calculated to investigate the similarity between the soil moisture products and ground observations.

Third, for evaluation of long term soil moisture estimates, soil moisture datasets were converted into Standardized Soil Moisture Index (SSMI) and were evaluated against the 1 month Standardized Precipitation Index (SPI-1; McKee et al., 1993) using 35 years of historical data measured at 101 ASOS stations for 1982–2016. In this study, the SPI-1 was used because of limited soil moisture measurements for a long period of records. The SPI on a time scale of 1–3 months gives the highest correlation with surface soil moisture whereas deeper soil layers show better correlation with longer time scales (Sims et al., 2002). Previous studies (Sur et al., 2015; Choi et al., 2013) demonstrated that the short term SPI shows similar spatial and temporal patterns as SSMI and can be used as a drought index in South Korea. Also, the short term SPI has been used to quantify agricultural droughts in other regions such as South America (Spennemann et al., 2015) and China (Li et al., 2018; Yuan et al., 2015).

Finally, probability of detection (POD), false alarm rate (FAR), and equitable threat score (ETS) were calculated to evaluate drought estimates from four soil moisture products against SPI-1 drought area from the gridded ASOS dataset (Wilks et al., 2011). Surface soil moisture is so responsive to precipitation that the precipitation based index can be used as independent drought evaluation. The drought condition is defined as the monthly SSMI and SPI-1 less than -0.8 (Yuan et al., 2015). This has the highest applicability in South Korea and corresponds to moderate drought (percentile < 20%) classified in the U.S. Drought Monitor (USDM; Svoboda et al., 2002). Also, we calculate the yearly drought area percentages for years 1982–2016 and compare the four soil moisture products at a basin scale.

3. Results and discussion

3.1. Evaluation of precipitation datasets

The GPCP and CHIRPS datasets are evaluated against the observation based precipitation ASOS dataset (OBS) in Fig. 1. In terms of the average annual precipitation rates for years 1982–2016, GPCP (1193 mm/yr) is lower than OBS (1268 mm/yr), but shows the similar spatial pattern as the OBS. CHIRPS shows the highest annual precipitation rates (1316 mm/yr) and represents higher rates particularly over southern and mid-eastern regions. Both domain-averaged temporal correlation coefficients of OBSvGPCP and OBSvCHIRPS are 0.95, but their spatial distributions are different (see Fig. 1d, 1e). The correlation coefficient map between ASOS and GPCP presents pointwise local patterns with lower values in areas near to ASOS precipitation stations (i.e. the "bulls-eye" features) due to its coarser resolution

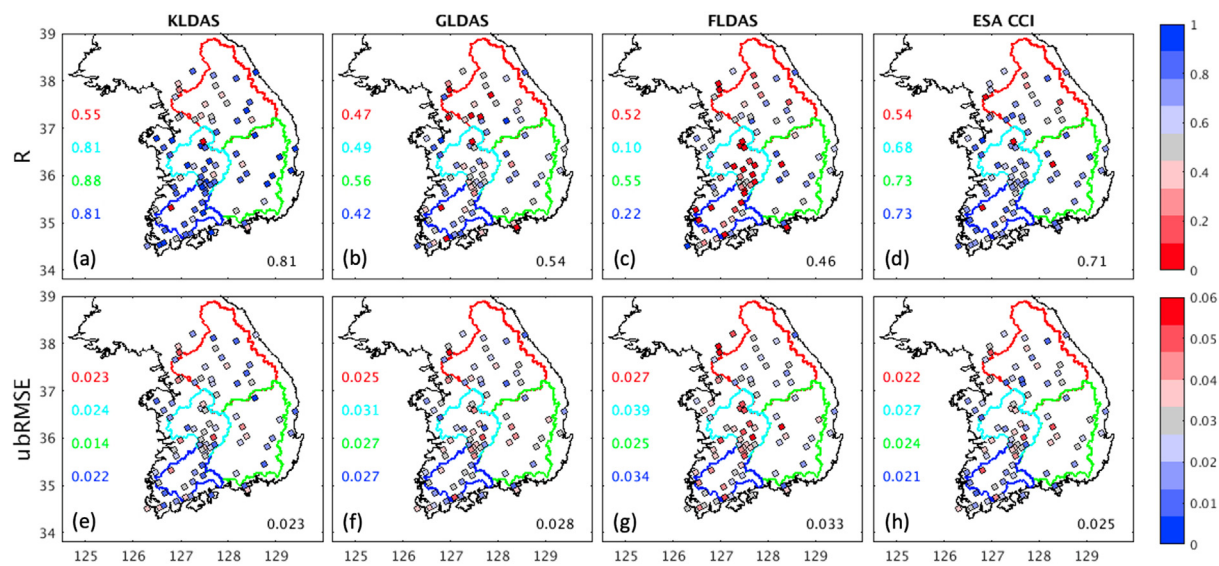


Fig. 2. Evaluation of soil moisture estimates from (a,e) KLDAS, (b,f) GLDAS, (c,g) FLDAS, and (d,h) ESC CCI against 78 in-situ observations for years 2013–2015. Black values are the domain-averaged anomaly R and anomaly RMSE metrics. Red, cyan, green and blue values and lines represent evaluation metrics and borders for each of four river basins, Han River basin over north, Geum River basin over west, Nakdong River basin over southeast, Yeongsan River basin over southwest of South Korea, respectively.

compared to CHIRPS. In terms of the average monthly precipitation rates, there are larger differences during wet seasons from July to August with almost half of the annual precipitation rates. The cumulative distribution functions (CDF) of three precipitation products (in Fig. 1g, 1h, 1i) are similar during spring (April to June), but shows the discrepancies during late summer (July to August) and early autumn (September to October). As a result, GLDAS forced by GPCP is likely to underestimate soil moisture whereas FLDAS forced by CHIRPS may overestimate soil moisture over the study area. This suggests that bias correction of the global precipitation datasets could improve their forced LSMs or hydrological models, particularly during wet season in South Korea.

3.2. Evaluation of soil moisture estimates

Soil moisture estimates from KLDAS, GLDAS, FLDAS, and ESA CCI are evaluated against 78 in situ observations between April and October during 2013–2015 in Fig. 2. Overall, KLDAS shows the best performance for all river basins in terms of anomaly R and anomaly RMSE metrics. The order of the evaluation metrics from highest to lowest is KLDAS, ESA CCI, GLDAS, and FLDAS. This supports that KLDAS at 0.01° spatial resolution better represents in situ soil moisture measurements than GLDAS at 0.25° resolution, FLDAS at 0.1° resolution, and ESA CCI at 0.25° resolution with the added value of local precipitation forcing dataset and soil texture maps. They provide more accurate and higher resolution datasets compared to the corresponding inputs to the other LDAS products. For example, soil texture maps from K-water accommodate more detailed categories of sandy loam (73%), clay loam (14%), and silty clay loam (5%) whereas the FAO's global soil texture maps occupy dominantly loam (96%).

Three additional Noah-MP experiments at 0.01° spatial resolution were carried out to separate out the effect of precipitation, soil texture, and downscaled meteorological forcing datasets on the KLDAS soil moisture estimates. Table 1 shows that an experiment without local precipitation and soil texture map (i.e. Ex3) outperforms the other LDAS soil moisture estimates by downscaling MERRA-2 meteorological forcing datasets through lapse-rate and slope-aspect correction methods and running the LSM at higher spatial resolution. Also, the local precipitation effect is larger than the local soil texture map when comparing the evaluation metric R and ubRMSE values of these

experiments. The KLDAS forced by both local precipitation and soil texture map shows the highest domain-averaged R value whereas the lowest domain-averaged ubRMSE value occurs in an experiment using only local precipitation dataset.

At a basin scale, the Nakdong River basin shows the highest R and lowest RMSE values than the other river basins except for RMSE in ESA CCI. This is related to the fact that, compared to the Nakdong River basin, the Han River basin is located over mixed forests and built-up areas and shows more spatial heterogeneity in soil moisture estimates. The Geum and Yeongsan River basins are mostly composed of cropland (i.e. rice paddy agriculture) where irrigated areas may not be well modeled for their regional irrigation rates. The KLDAS, GLDAS, and FLDAS products used in this study do not consider irrigation modules in the modeling framework to generate their hydrological variables.

3.3. Evaluation of standardized soil moisture index

Monthly SSMI maps from the four soil moisture products are evaluated against monthly SPI-1 from the ASOS precipitation dataset for 1982–2016 in South Korea where long term records of in situ soil moisture measurements are limited. Fig. 3 represents the spatial distribution maps of the SSMI and SPI-1 values for a recent May 2015 drought event in South Korea. Overall, SSMI maps show dry status with negative values in northern South Korea and relatively wet status in southern South Korea. The SPI-1 maps from the ASOS observations, GPCP, and CHIRPS were expected to show the similar spatial pattern of the SSMI maps from KLDAS, GLDAS, and FLDAS, respectively. This supports that despite the similar LSMs (used in the three LDAS products) and the same MERRA-2 forcing dataset (used in the two LDAS products), changes in precipitation can serve as the main driver of the modeled soil moisture variability. It is noteworthy that most products show the May 2015 drought condition in the central region, but the GLDAS and ESA CCI products present mild conditions. Compared to GLDAS and ESA CCI, FLDAS seems to better capture the May 2015 drought with the similar spatial pattern as the KLDAS map.

Fig. 4 shows the correlation coefficients between the ASOS SPI-1 and each of the four monthly SSMIs for 1982–2016. The order of the evaluation metric from highest to lowest is KLDAS, GLDAS, FLDAS, and ESA CCI. KLDAS shows the best result, which is in agreement with evaluation of soil moisture estimates in Fig. 2. But, the lowest

Table 1

Comparison of evaluation metrics R and ubRMSE for four experiments at 0.01° spatial resolution against in-situ soil moisture observations for years 2013–2015. The best results in each region are in boldface.

Experiments	KLDAS*- rainfall (ASOS)- Soil (K-water)	Ex1 - rainfall (ASOS)- Soil (FAO)	Ex2 - rainfall (MERRA-2)- Soil (K-water)	Ex3 - rainfall (MERRA-2)- Soil (FAO)				
Evaluation metrics	R	ubRMSE	R	ubRMSE	R	ubRMSE	R	ubRMSE
Domain-avg.	0.81	0.023	0.79	0.021	0.77	0.025	0.72	0.023
Han R.	0.55	0.023	0.54	0.018	0.46	0.026	0.47	0.020
Geum R.	0.81	0.024	0.79	0.023	0.75	0.028	0.66	0.026
Nakdong R.	0.88	0.014	0.92	0.015	0.83	0.016	0.93	0.016
Yeongsan R.	0.81	0.022	0.80	0.023	0.78	0.023	0.72	0.026

*Results are shown in Fig. 2a, 2e.

performance is found in ESA CCI with the second best in Fig. 2. This indicates that though ESA CCI better captures recent soil moisture behavior, it is not feasible to detect historical drought conditions. This can be related to the fact that the quality of ESA CCI product depends on the quality of the data used in its algorithm. The ESA CCI products with more recent satellite observations can provide improved soil moisture estimates along with an increase of the spatio-temporal coverages. Note that only a single passive microwave retrieval was used to produce soil moisture estimates in the early period (1979–1991) of the ESA CCI merged product (Dorigo et al., 2015; McNally et al., 2016). Interestingly, KLDAS presents more detailed spatial patterns due to higher resolution soil texture maps as the model inputs. The border between North and South Korea at latitudes 38–39° appears with a coarser spatial scale as a result of the coarser soil texture maps and lower precipitation sampling rates compared to the domain of South Korea. GLDAS and EAS CCI show the lowest performance in the midwestern region, particularly with the “bulls-eye” pattern in GLDAS. This localized lower performance is found in the Seoul metropolitan area, a location with heterogeneous land cover. This can be also explained by the fact that these two coarser global products are limited to capture local scale spatiotemporal variability of hydrological variables. At a basin scale, the Yeongsan River basin shows the highest R values in KLDAS and ESA CCI, but the lowest values in GLDAS product, which is similar to the results in Fig. 2.

The correlation coefficients between the ASOS SPI-1 and each of the four monthly SSMIs are calculated by months from April to October in Fig. 5. Overall, all soil moisture products show similar R values in both dry and wet seasons. KLDAS shows higher R values (> 0.6) during all

crop growing seasons with lower standard deviations than the other soil moisture products. This supports that their agricultural drought estimates have little seasonal variation and bias, which can be useful to monitor droughts during all crop growing seasons between April and October.

3.4. Evaluation of drought estimates

The spatial maps of probability of detection (POD), false alarm rate (FAR), and equitable threat score (ETS) for monthly agricultural drought estimates are calculated in Fig. 6. Monthly agricultural droughts (SSMI less than −0.8) detect ~50% of monthly precipitation droughts (SPI-1 less than −0.8) over South Korea with an average POD of 0.45–0.67 and ETS of 0.19–0.43 in the four major river basins except for ESA CCI. The order of evaluation metrics POD and ETS from highest to lowest is KLDAS, GLDAS, FLDAS, and ESA CCI, which follows the same order of the SSMI evaluation in Fig. 4. It is noteworthy that GLDAS outperforms EAS CCI products with the same spatial resolution and shows the similar performance as FLDAS at a higher spatial resolution in evaluation of drought estimates. Compared to FAR, both POD and ETS show more similar spatial patterns at a basin scale. The order of basins from highest to lowest in evaluation of drought estimates are different from the results in Figs. 2 and 4. This can be explained by the fact that the evaluations of soil moisture products and their SSMI indices include the whole range of values, but this evaluation of drought estimates consider only a range of the lowest values.

Time series of the drought area percentages are calculated for each of the four river basins for 1982–2016 in Fig. 7. The drought area

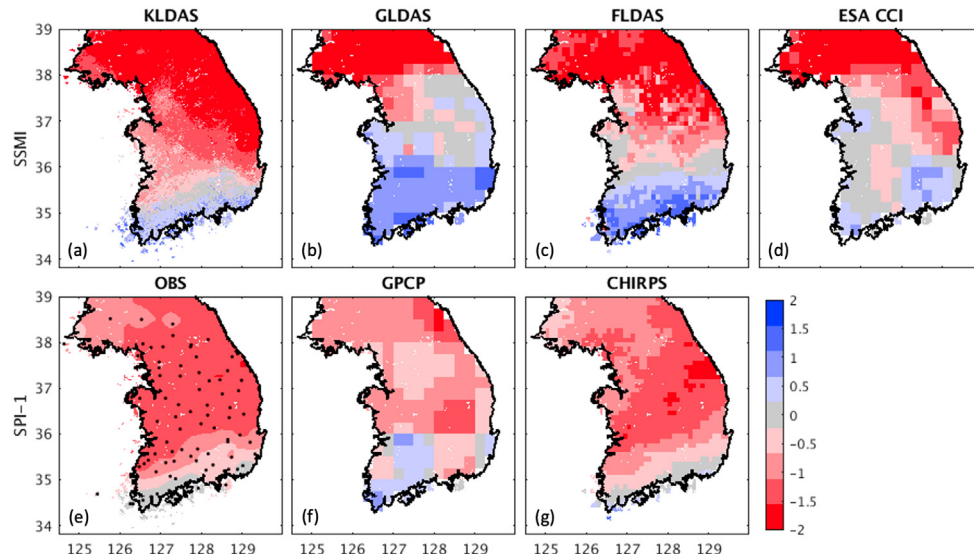


Fig. 3. A recent drought event over South Korea in May 2015. (a-d) Monthly standardized soil moisture indices (SSMI), (e-g) one month standardized precipitation indices (SPI-1).

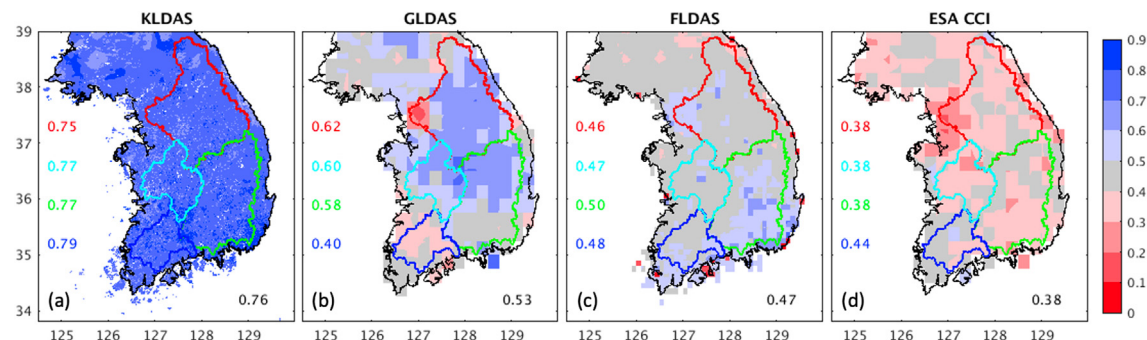


Fig. 4. The spatial maps of correlation coefficients between monthly standardized precipitation indices (SPI-1) and each of the four monthly standardized soil moisture indices (SSMI) for 1982–2016.

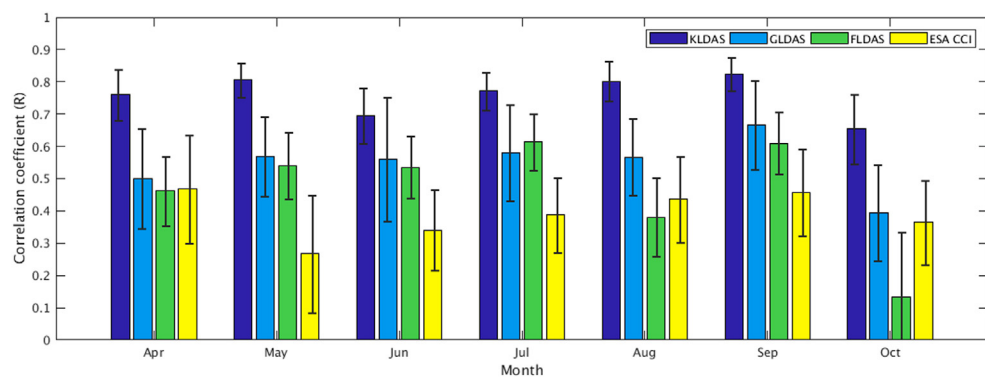


Fig. 5. Bar graphs of the correlation coefficients between SSMI and SPI-1 by month from April to October. Error bars indicate ± 1 standard deviation.

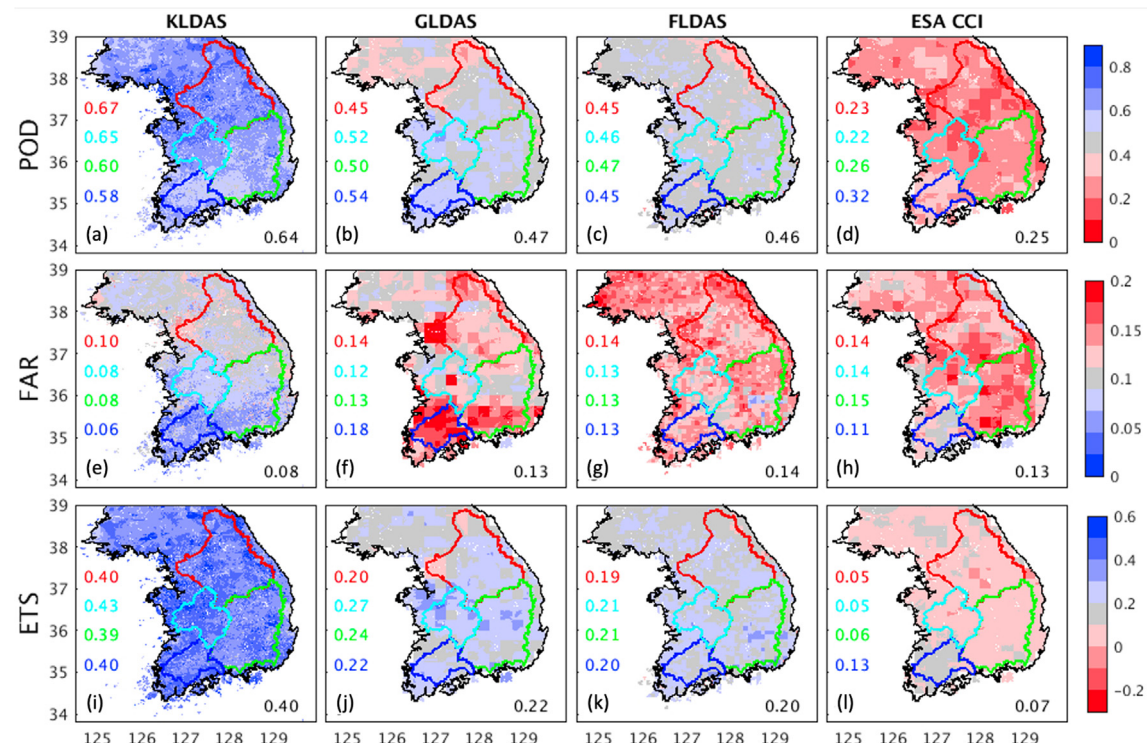


Fig. 6. Probability of detection (POD), false alarm rate (FAR), and equitable threat score (ETS) for monthly agricultural droughts between April and October during 1982–2016.

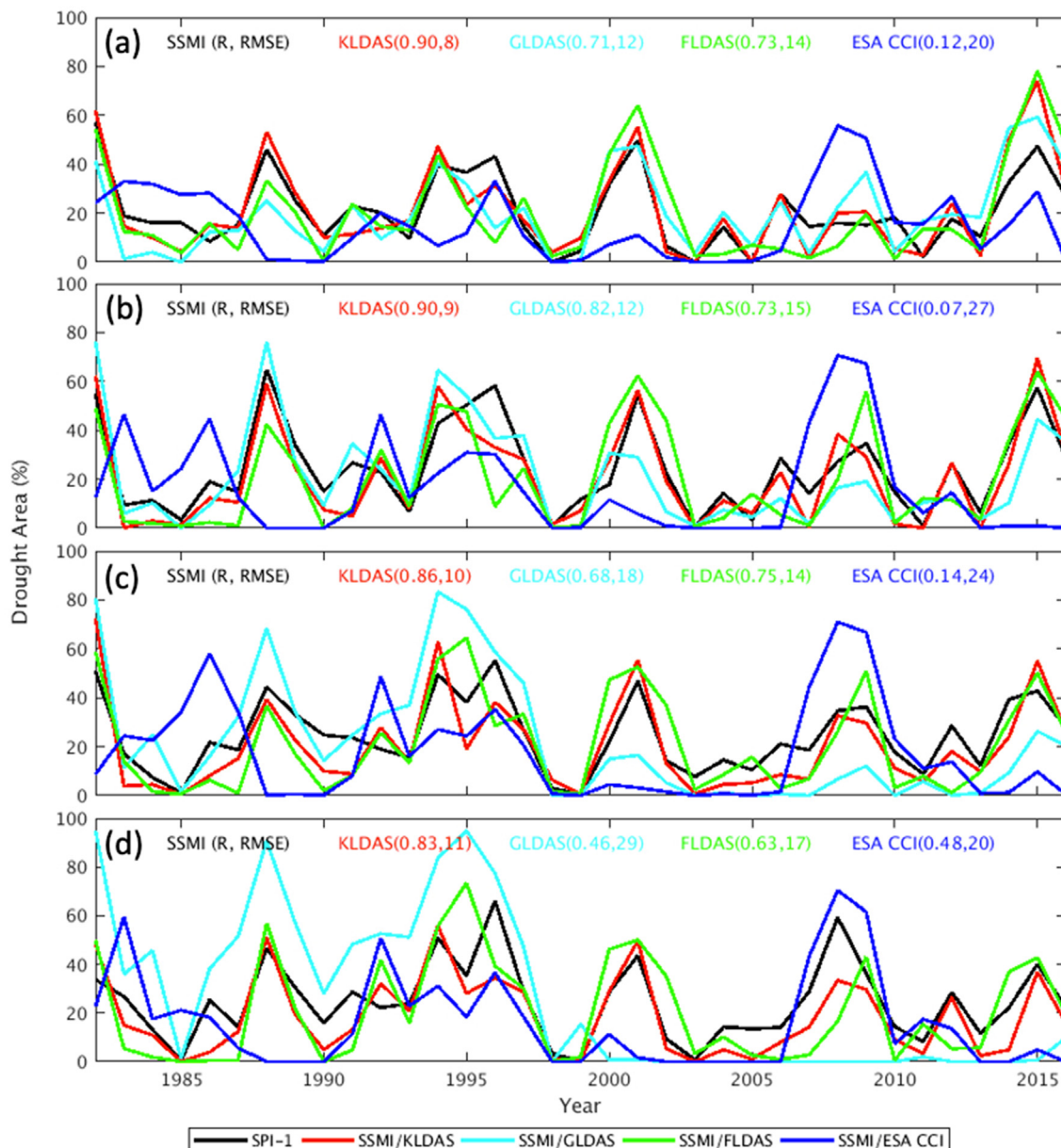


Fig. 7. Time series of the drought area percentages for each of four river basins, (a) Han River basin over north, (b) Geum River basin over west, (c) Nakdong River basin over southeast, (d) Yeongsan River basin over southwest of South Korea. The values are correlation coefficient (R) and root-mean-square error (RMSE) metrics between SPI-1 and SSMI based drought percentage areas.

percentages from the four soil moisture products are evaluated against the ASOS SPI-1 in terms of R and RMSE values. As expected, KLDAS shows the best performance in all river basins. The order of evaluation metrics R and RMSE from highest to lowest is the similar order as both evaluations in Figs. 4 and 6, but FLDAS slightly outperforms GLDAS except in the Geum River basin. Overall, KLDAS and FLDAS provide higher R (> 0.63) and lower RMSE ($< 17\%$) values in all four river basins. It is interesting to note that overestimation of the agricultural drought areas is found in the Nakdong River and Yeongsan River basins during 1982–200 in the GLDAS products, which leads to produce lower performance than the other Han River and Geum River basins.

All four major river basins also appear to experience periodic droughts, related to the impact of regional monsoon circulation over the East Asia. SSMI from KLDAS shows that these basins have wet status with lower drought area percentages ($< 20\%$) for years 1983–1987, 1990–1991, 1993, 1998–1999, 2002–2007, 2010–2011, 2013 and dry status with higher drought area percentages ($> 40\%$) for years 1982,

1988, 1994, 2001, 2015. In Fig. 7, the most recent 2015 drought event leads to the highest drought area percentage 74% of the Han River basin and 69% of the Geum River basin in the past 35 years for our study period.

4. Conclusions

Regional land surface models are required to facilitate continuous hydrological monitoring for the analysis of droughts and their characteristics of spatial variation, intensity and frequency under climate change. But, model-based soil moisture has not been fully served as an agricultural drought index to monitor long term drought conditions in South Korea. In this study, we describe the development of a 0.01° resolution LDAS using the Noah-MP model with the added value of local precipitation forcing dataset and high-resolution soil texture maps in South Korea where rugged topography and heterogeneous land covers make coarse resolution LSM and satellite retrieval difficult to

capture agricultural droughts. This study examines the potential of KLDAS soil moisture estimates for long term drought monitoring during crop growing seasons for 1982–2016. The KLDAS soil moisture estimates are evaluated using two reference datasets: 3-year in situ soil moisture measurements and 35-year observed precipitation-based SPI-1. Also, we employ GLDAS, FLDAS and ESA CCI as benchmark datasets and intercompare them with KLDAS because these soil moisture products have been investigated for good quality drought monitoring in other regions. These datasets are the only available resource to provide long term soil moisture estimates over South Korea.

KLDAS outperforms the benchmark soil moisture estimates and their drought estimates in South Korea. For drought detectability, KLDAS has higher POD and ETS than the other LDAS and satellite retrieval products in all four major river basins. The GPCP (used to force GLDAS) and CHIRPS (used to force FLDAS) datasets are under- and overestimated than the observation based ASOS dataset in South Korea for 1982–2016, particularly during wet seasons. The GLDAS and ESA CCI products show the lowest performance in the metropolitan area with heterogeneous land covers. This work suggests that improved precipitation, soil texture maps, and model spatial resolution are crucial for agricultural drought estimation over South Korea. ESA CCI shows the second best in the recent soil moisture estimates against in situ measurements for a shorter period of time (2013–2015). But, our results indicate that the ESA CCI products are not feasible for long term drought monitoring over South Korea due to lower data quality for early periods (1979–1991) of the ESA CCI merged product. From a basin scale perspective, the Nakdong River basin in the southeast of South Korea shows the best results in the soil moisture estimation for 2013–2015 because the mid-eastern region is high in elevation with rugged topography and the western and southern regions are more occupied with cropland where irrigation modules need to be considered, but were not included by any of these LDAS products.

Improved forcing datasets and additional model development can meet the full potential of the KLDAS as agricultural drought monitoring tools. Currently, the other ASOS meteorological forcing datasets (i.e. wind, air temperature, pressure, humidity) than the precipitation are being processed into a 0.01° gridded data and are set to force high resolution KLDAS coupled with a river routing scheme (Getirana et al., 2012, 2017). Assimilating land surface data into LSMs can improve poorly represented processes over irrigated and vegetation-covered areas (Kumar et al., 2015; Jung et al., 2019), which cannot be supported by simpler models and ground observation-based SPI and SSMI approaches. In addition to the enhanced drought monitoring system, KLDAS is expected to provide important information on water resources as a valuable tool for key stakeholders to manage natural resources and develop water supply guidelines and best practices in South Korea.

CRediT authorship contribution statement

Hahn Chul Jung: Writing - original draft, Conceptualization, Methodology, Validation. **Do-Hyuk Kang:** Conceptualization, Writing - review & editing, Validation. **Edward Kim:** Supervision, Writing - review & editing. **Augusto Getirana:** Conceptualization, Methodology, Writing - review & editing. **Yeosang Yoon:** Methodology, Validation. **Sujay Kumar:** Methodology, Writing - review & editing. **Christa D. Peters-Lidard:** Supervision, Writing - review & editing. **EuiHo Hwang:** Supervision.

Declaration of Competing Interest

The authors declare that they have no known competing financial interests or personal relationships that could have appeared to influence the work reported in this paper.

Acknowledgments

This research was supported by Korea Environment Industry and technology Institute through Water Management Research Program, funded by Korea Ministry of Environment (grant number: 79622). Computing was supported by the resources at the NASA Center for Climate Simulation (NCCS). The GLDAS and FLDAS data were provided by NASA's Earth Science Division and distributed by the Goddard Earth Sciences (GES) Data and Information Services Center (DISC) (<https://disc.gsfc.nasa.gov>). The CCI SM products were made available from ESA CCI website (<https://www.esa-soilmoisture-cci.org>).

References

- Adler, R.F., et al., 2003. The version-2 Global Precipitation Climatology Project (GPCP) monthly precipitation analysis (1979–present). *J. Hydrometeorol.* 4, 1147–1167.
- Albergel, C., Rüdiger, C., Pellarin, T., Calvet, J.C., Fritz, N., Froissard, F., Suquia, D., Pettipa, A., Piguet, B., Martin, E., 2008. From near-surface to root-zone soil moisture using an exponential filter: An assessment of the method based on in-situ observations and model simulations. *Hydro. Earth Syst. Sci.* 12, 1323–1337.
- Anderson, M.C., Hain, C., Otkin, J., Zhan, Z., et al., 2013. An Intercomparison of Drought Indicators Based on Thermal Remote Sensing and NLDAS-2 Simulations with U.S. Drought Monitor Classifications. *J. Hydrometeorol.* 14, 1035–1056.
- Anderson, M.C., Hain, C., Wardlow, B., Pimstein, A., Mecikalski, J.R., Kustas, W.P., 2011. Evaluation of Drought Indices Based on Thermal Remote Sensing of Evapotranspiration over the Continental United States. *J. Hydrometeorol.* 24, 2025–2044.
- Cai, X., Yang, Z.-L., David, C.H., Niu, G.-Y., Rodell, M., 2014. Hydrological evaluation of the Noah-MP land surface model for the Mississippi River Basin. *J. Geophys. Res. Atmos.* 119, 23–38.
- Chaney, N.W., Roundy, J.K., Herrera-Estrada, J.E., Wood, E.F., 2015. High-resolution modeling of the spatial heterogeneity of soil moisture: Applications in network design. *Water Resour. Res.* 51, 619–638.
- Choi, M., Jacobs, J.M., Anderson, M.C., Bosch, D.D., 2013. Evaluation of Drought Indices via Remotely Sensed Data with Hydrological Variables. *J. Hydrol.* 476, 265–273.
- Derber, J.C., Parrish, D.F., Lord, S.J., 1991. The new global operational analysis system at the National Meteorological Center. *Wea. Forecasting* 6, 538–547.
- Dorigo, W.A., Gruber, A., de Jeu, R.A.M., Wagner, W., Stacke, T., Loew, A., Kidd, R., 2015. Evaluation of the ESA CCI soil moisture product using ground-based observations. *Remote Sens. Environ.* 162, 380–395.
- Friedl, M., McIver, D., Hodges, J., Zhang, X., Muchoney, D., Strahler, A., et al., 2002. Global land cover mapping from MODIS: algorithms and early results. *Remote Sens. Environ.* 83, 287–302.
- Funk, C., Peterson, P., Landsfeld, M., Pedreros, D., Verdin, J., Shukla, S., Husak, G., Rowland, J., Harrison, L., Hoell, A., et al., 2015. The climate hazards infrared precipitation with stations—A new environmental record for monitoring extremes. *Sci. Data* 2, 150066.
- Getirana, A.C.V., Boone, A., Yamazaki, D., Decharme, B., Papa, F., Mognard, N., 2012. The hydrological modeling and analysis platform (HyMAP): evaluation in the Amazon basin. *J. Hydrometeorol.* 13, 1641–1665.
- Getirana, A., Peters-Lidard, C., Rodell, M., Bates, P.D., 2017. Trade-off between cost and accuracy in large-scale surface water dynamic modeling. *Water Resour. Res.* 53, 4942–4955.
- Gutman, G., Ignatov, A., 1998. The derivation of the green vegetation fraction from NOAA/AVHRR data for use in numerical weather prediction models. *Int. J. Remote Sens.* 19, 1533–1543.
- Hong, I., Lee, J.H., Cho, H.S., 2016. National drought management framework for drought preparedness in Korea (lessons from the 2014–2015 drought). *Water Policy* 18, 89–106.
- Jackson, T.J., Cosh, M.H., et al., 2010. Validation of Advanced Microwave Scanning Radiometer soil moisture products. *IEEE Trans. Geosci. Remote Sens.* 48, 4256–4272.
- Jang, D., 2018. Assessment of Meteorological Drought Indices in Korea Using RCP 8.5 Scenario. *Water* 10, 283. <https://doi.org/10.3390/w10030283>.
- Jung, H.C., Getirana, A., Arsenault, K.R., Sujay, K., Maigary, I., 2019. Improving Surface Soil Moisture Estimates in West Africa through GRACE Data Assimilation. *J. Hydrol.* 2575, 192–201.
- Jung, C., Lee, Y., Cho, Y., Kim, S., 2017. A study of spatial soil moisture estimation using a multiple linear regression model and MODIS land surface temperature data corrected by conditional merging. *Remote Sens.* 9. <https://doi.org/10.3390/rs9080870>.
- Koster, R.D., Guo, Z., Yang, R., Dirmeyer, P., Mitchell, K., Puma, M.J., 2009. On the nature of soil moisture in land surface models. *J. Clim.* 22, 4322–4335.
- Kumar, S.V., Peters-Lidard, C.D., Mocko, D., et al., 2014. Assimilation of remotely sensed soil moisture and snow depth retrievals for drought estimation. *J. Hydrometeorol.* 15, 2446–2469.
- Kumar, S.V., Peters-Lidard, C.D., Mocko, D., Tian, Y., 2013. Multiscale evaluation of the improvements in surface snow simulation through terrain adjustments to radiation. *J. Hydrometeorol.* 14, 220–232.
- Kumar, S.V., Peters-Lidard, C.D., Santanello, J.A., et al., 2015. Evaluating the utility of satellite soil moisture retrievals over irrigated areas and the ability of land data assimilation methods to correct for unmodeled processes. *Hydro. Earth Syst. Sci.* 19, 4463–4478.

- Kwon, H.H., Lall, U., Kim, S.J., 2016. The unusual 2013–2015 drought in South Korea in the context of a multicentury precipitation record: Inferences from a nonstationary, multivariate, Bayesian copula model. *Geophys. Res. Lett.* 43, 8534–8544. <https://doi.org/10.1002/2016GL070270>.
- Li, Y., Li, Y., Yuan, X., Zhang, L., Sha, S., 2018. Evaluation of Model-Based Soil Moisture Drought Monitoring over Three Key Regions in China. *J. Appl. Meteor. Climatol.* 57, 1989–2004.
- Loew, A., Stacke, T., Dorigo, W., de Jeu, R., Hagemann, S., 2013. Potential and limitations of multidecadal satellite soil moisture observations for selected climate model evaluation studies. *Hydroclim. Sci.* 17, 3523–3542.
- McKee, T.B.; Doesken, N.J.; Kleist, J. The relationship of drought frequency and duration to time scales. Preprints, in Eighth Conf. on Applied Climatology, 1993, 179–184, Am. Meteorol. Soc., Anaheim, Calif.
- McNally, A., et al., 2016. Evaluating ESA CCI soil moisture in East Africa. *Int. J. Appl. Earth Observat. Geoinformat.* 48, 96–109.
- McNally, A., Arsenault, K., Kumar, S., Shukla, S., Peterson, P., Wang, S., Funk, C., Peters-Lidard, C.D., Verdin, J.P., 2017. A land data assimilation system for sub-Saharan Africa food and water security applications. *Scientific Data*. 4. <https://doi.org/10.1038/sdata.2017.12>.
- Ministry of Agriculture, Food and Rural Affairs (MAFRA), Statistical yearbook of land and water development for agriculture 2016, Korea Rural Community Corporation, Rural Research Institute, 2017, Ansan, Korea.
- Mitchell, K.E., et al., 2004. The multi-institution North American Land Data Assimilation System (NLDas): Utilizing multiple GCIP products and partners in a continental distributed hydrological modeling system. *J. Geophys. Res.* 190, D07S90. <https://doi.org/10.1029/2003JD003823>.
- Niu, G.-Y., Yang, Z.-L., Dickinson, R.E., Gulden, L.E., Su, H., 2007. Development of a simple groundwater model for use in climate models and evaluation with Gravity Recovery and Climate Experiment data. *J. Geophys. Res.* 112, D07103. <https://doi.org/10.1029/2006JD007522>.
- Park, S., Im, J., Park, S., Rhee, J., 2017. Drought monitoring using high resolution soil moisture through multi-sensor satellite data fusion over the Korean peninsula. *Agricul. Forest Meteorol.* 257–269.
- Pietroniro, A., Prowse, T.D., 2002. Applications of remote sensing in hydrology. *Hydroclim. Process.* 16, 1537–1541.
- Reichle, R.H., Liu, Q., Koster, R.D., Draper, C.S., Mahanama, S.P.P., Partyka, G.S., 2017. Land surface precipitation in MERRA-2. *J. Clim.* 30, 1643–1664.
- Reynolds, C.A., Jackson, T.J., Rawls, W.J., 2000. Estimating soil water-holding capacities by linking the food and agriculture organization soil map of the world with global pedon databases and continuous pedotransfer functions. *Water Resour. Res.* 36, 3653–3662.
- Rodell, M., Houser, P.R., Jambor, U., Gottschalck, J., Mitchell, K., Meng, C.-J., Arsenault, K., Cosgrove, B., Radakovich, J., Bosilovich, M., Entin, J.K., Walker, J.P., Lohmann, D., Toll, D., 2004. The Global Land Data Assimilation System. *Bull. Amer. Meteor. Soc.* 85, 381–394.
- Rodriguez, E.; Morris, C.; Belz, J.; Chapin, E.; Martin, J.; Daffer, W. et al. An assessment of the SRTM topographic products. Technical Report JPL, 2005, D-31639, Jet Propulsion Laboratory, Pasadena, CA.
- Ryu, J.H., Han, K.S., Lee, Y.W., Park, N.W., Hong, S., Chung, C.Y., Cho, J., 2019. Different agricultural responses to extreme drought events in neighboring counties of South and North Korea. *Remote Sens.* 11, 1773. <https://doi.org/10.3390/rs11151773>.
- Sheffield, J., Wood, E.F., 2007. Characteristics of global and regional drought, 1950–2000: Analysis of soil moisture data from off-line simulation of the terrestrial hydrologic cycle. *J. Geophys. Res.* 112, D17115. <https://doi.org/10.1029/2006JD008288>.
- Sheffield, J., Goteti, G., Wood, E.F., 2006. Development of a 50-year high-resolution global dataset of meteorological forcings for land surface modeling. *J. Clim.* 19, 3088–3111.
- Sims, A.P., Niyogi, D.S., Raman, S., 2002. Adopting drought indices for estimating soil moisture: A North Carolina case study. *Geophys. Res. Lett.* 29, 1183. <https://doi.org/10.1029/2001GL013343>.
- Spennemann, P.C., Rivera, J.A., Saulo, A.C., Penalba, O.C., 2015. A comparison of GLDAS soil moisture anomalies against standardized precipitation index and multisatellite estimations over South America. *J. Hydrometeorol.* 16, 158–171.
- Sur, C., Hur, J., Kim, K., Choi, W., Choi, M., 2015. An evaluation of satellite-based drought indices on a regional scale. *Int. J. Remote Sens.* 36, 5593–5612.
- Svoboda, M.; Coauthors.. The Drought Monitor. *Bull. Amer. Meteor. Soc.*, 2002, 83, 1181–1190.
- Wilks, D.S. Statistical Methods in the Atmospheric Sciences, Int. Geophys. Ser., 2011, 100, 676 , Academic Press, San Diego, Calif.
- Yoon, D.H., Nam, W.H., Lee, H.J., Hong, E.M., Feng, S., Wardlow, F.B., Tadesse, T., Svoboda, M.D., Hayes, M.J., Kim, D.E., 2020. Agricultural drought assessment in East Asia using satellite-based indices. *Remote Sens.* 12, 444. <https://doi.org/10.3390/rs12030444>.
- Yuan, X., Ma, Z., Pan, M., Shi, C., 2015. Microwave remote sensing of short-term droughts during crop growing seasons. *Geophys. Res. Lett.* 43, 4394–4401.